Functional Characterization of the Secondary Actin Binding Site of Myosin II[†]

Juliette Van Dijk,[‡,§] Marcus Furch,[‡,‖] Chrystel Lafont,[§] Dietmar J. Manstein,[‖] and Patrick Chaussepied*,[§]

Centre de Recherche de Biochimie Macromolèculaire du Centre National de la Recherche Scientifique, Institut Féderatif de Recherche 24, Montpellier, France, and Max-Planck-Institut für Medizinische Forschung, Heidelberg, Germany

Received July 9, 1999; Revised Manuscript Received August 31, 1999

ABSTRACT: The role of the interaction between actin and the secondary actin binding site of myosin (segment 565–579 of rabbit skeletal muscle myosin, referred to as loop 3 in this work) has been studied with proteolytically generated smooth and skeletal muscle myosin subfragment 1 and recombinant *Dictyostelium discoideum* myosin II motor domain constructs. Carbodiimide-induced cross-linking between filamentous actin and myosin loop 3 took place only with the motor domain of skeletal muscle myosin and not with those of smooth muscle or *D. discoideum* myosin II. Chimeric constructs of the *D. discoideum* myosin motor domain containing loop 3 of either human skeletal muscle or nonmuscle myosin were generated. Significant actin cross-linking to the loop 3 region was obtained only with the skeletal muscle chimera both in the rigor and in the weak binding states, i.e., in the absence and in the presence of ATP analogues. Thrombin degradation of the cross-linked products was used to confirm the cross-linking site of myosin loop 3 within the actin segment 1–28. The skeletal muscle and nonmuscle myosin chimera showed a 4–6-fold increase in their actin dissociation constant, due to a significant increase in the rate for actin dissociation (k_{-A}) with no significant change in the rate for actin binding (k_{+A}). The actin-activated ATPase activity was not affected by the substitutions in the chimeric constructs. These results suggest that actin interaction with the secondary actin binding site of myosin is specific for the loop 3 sequence of striated muscle myosin isoforms but is apparently not essential either for the formation of a high affinity actin–myosin interface or for the modulation of actomyosin ATPase activity.

Myosin molecules are actin-based molecular motors that use the energy supplied by the hydrolysis of ATP to perform various cell motility processes. The catalytic activity of myosin resides in its conserved motor domain, which interacts with actin, binds to and hydrolyzes ATP, and produces the force necessary for movement along actin filaments. Although the 3-D structure of the motor domain is highly conserved within the myosin family (*1*, *2*), the enzymatic and motile activities of different myosin isoforms show a high degree of divergence (*3*). These functional variations are probably not due to fundamental differences in the molecular mechanism used by each isotype to convert the chemical energy into mechanical force but rather reflect a fine-tuning to specific functional requirements that is brought about by variations in the primary sequence of the motor domain itself. In agreement with this idea, sequence alignments reveal large differences in primary sequence at the proposed actin–myosin interface (*4*). Within this interface, one can clearly distinguish electrostatic and hydrophobic contacts (*5*, *6*). The formation of the initial collision complex formed in the presence of ATP and ADP·P$_i$ is largely an ionic interaction, whereas the transition from the weak to the strong binding complex has both ionic and hydrophobic characteristics (*7*–*11*). Both 3-D reconstructions of electron microscopic images and solution experiments performed on the actomyosin complex have suggested two main electrostatic binding sites. These sites encompass a patch of negative charges located on subdomain 1 of two adjacent actin monomers and two positively charged surface loops of skeletal muscle myosin residues 626–647 (loop 2) and residues 565–579, referred to as loop 3 for simplicity in the remainder of this paper. Note that loop 1 (residues 204–216 of skeletal muscle myosin) is not involved in actin binding (*5*) but only in the regulation of ATP turnover rates by modulating ADP release (*12*–*14*).

Since both loops (2 and 3) are highly divergent in length and in charge content in the myosin family (*3*, *4*), they were suggested to play a role in determining functional characteristics of myosins (*15*, *16*). Biochemical and molecular genetic studies with chimeric proteins have clearly demonstrated that loop 2 tunes the catalytic efficiency of the different myosin isotypes (*17*–*22*). Similar to the docking process of other protein–protein interfaces (*23*, *24*), the association rate of myosin and actin is governed by the number of charges present in loop 2 (*20*).

Less is known about the role of loop 3 in modulating the activity of the actomyosin complex. Experiments performed both in solution (under nonsaturating conditions) and in myofibrils showed that loop 3 of skeletal or cardiac muscle myosin can be cross-linked to (interacts with) the N-terminus of actin (*25*–*27*). This interaction is supported by the fact

* Corresponding author: CRBM du CNRS, 34293 Montpellier Cédex 5, France; tel (33) 4 67 61 33 34; Fax (33) 4 67 52 15 59; email chaussepied@crbm.cnrs-mop.fr.
‡ J.V.D. and M.F. contributed equally to this work.
§ CRBM du CNRS.
‖ Max-Planck-Institut für Medizinische Forschung.

that proteolytic cleavage of loop 3 inhibits the actin-activated ATPase activity of both rabbit skeletal and scallop muscle myosin (*28, 29*). Moreover, an antipeptide antibody directed against loop 3 of skeletal muscle myosin has a strong inhibitory effect on the sliding velocity of actin filaments in an in vitro motility assay (*30*). On the other hand, cross-linking reactions with smooth muscle myosin (*31*) or *Dictyostelium discoideum* myosin (*21*) did not provide evidence for an interaction between myosin loop 3 and actin. Only a mutation of *D. discoideum* myosin loop 3 (Arg562 to Leu) was found to impair its actin-activated ATPase activity, suggesting at least an indirect link between loop 3 and the actin interface in nonmuscle actomyosin (*32*).

To determine the involvement of loop 3 in the catalytic specificity of myosin isoforms, we have compared the actin binding properties of five myosin motor domains containing different loop 3 sequences: two myosin subfragments 1 prepared by chymotrypsin and papain cleavage of skeletal and smooth muscle myosin, respectively; the *D. discoideum* myosin motor domain; and two chimeric constructs of the *D. discoideum* myosin motor domain containing loop 3 of human skeletal muscle or nonmuscle myosin. Using carbodiimide-induced cross-linking, we found that significant actin cross-linking to the secondary actin binding site is obtained only with the motor domains containing skeletal muscle myosin loop 3. Moreover, quantitative analyses of the actin binding and actin-activated ATPase properties of the different motor domains favor a relatively weak role of loop 3 in the formation and the activity of the actomyosin complex.

MATERIALS AND METHODS

Materials. Trypsin, thrombin from human plasma (200 units/mg), papain, ADP, phalloidin, 1-ethyl-3-[3-(dimethyl-amino)propyl]carbodiimide (EDC),[1] and *N*-hydroxysuccin-imide (NHS) were purchased from Sigma. NaF, BeSO$_4$, and AlCl$_3$ were from Merck. Soybean trypsin inhibitor and ATP were obtained from Boehringer Mannheim. Chymotrypsin and *N*-(1-pyrenyl)iodoacetamide were from Worthington Biochemicals and Molecular Probes, respectively. Sephacryl 200 was supplied by Pharmacia. All other chemicals were of analytical grade.

Preparation of Proteins. Rabbit skeletal filamentous actin was prepared from acetone powder and further purified by two cycles of polymerization−depolymerization (*33*). Skeletal muscle myosin subfragment 1 (Sk-S1) was prepared from rabbit muscle after chymotryptic digestion of myosin filaments (*34, 35*). Sk-S1 carrying the alkali light chain 2 was prepared by ion-exchange chromatography as described previously (*36*). Smooth muscle myosin subfragment 1 (Sm-

S1) was prepared after papain degradation of chicken gizzard muscle myosin as reported (*37*). Recombinant myosin head fragments were expressed in *D. discoideum* and purified as described by Manstein and Hunt (*38*). Standard procedures (*39*) were followed for the production of two chimeric contructs, M765(Sk) and M765(NM), starting with the extrachromosomal vector pDH20 (*20*). pDH20 contains sequence coding for the first 765 residues of the *D. dicoideum mhc*A gene fused to a C-terminal His$_8$ tag under the control of the *D. discoideum* actin 15 promoter. The following mutagenic primers were used in a PCR described by Braman et al. (*40*) (mutated nucleotides are underlined): M765(Sk), 5′-CAAATACCAAAAACCAAAGGTTGTTAAGGGTAAA-GCTGAGACCGAATTTGGTGTTACC and 5′-GGTAA-CACCAAATTCGGTCTCAGCTTTACCCTTAACAACCTT-TGGTTTTTGGTATTTG; M765(NM), 5′-CAAGAAGAAC-GCCAAATACCAAAAACCAAAGCAACTTAAGGATAAAA-CCGAATTTGGTGTTACC and 5′-GGTAACACCAAAT-TCGGTTTTATCCTTAAGTTGCTTTGGTTTTTGGTATTT-GGCGTTCTTCTTG. The new plasmids were named pDH20sk and pDH20nm, respectively. Each DNA construct was confirmed by sequencing to ensure that the desired mutation had been introduced.

Protein concentrations were determined spectrophotometri-cally by use of the extinction coefficients of $A^{1\%}_{280nm} = 11$ cm^{-1} for actin (*41*), 5.7 cm^{-1} for skeletal muscle myosin (*42*), 7.5 cm^{-1} for Sk-S1 (*43*), and 4.5 cm^{-1} for smooth muscle myosin (*44*). The concentration of Sm-S1 and *D. discoideum* motor domains were estimated by Bradford's method (*45*). The molecular masses used were 42, 500, 115, 135, and 88 kDa for actin, skeletal and smooth muscle myosin, Sk-S1, Sm-S1, and M765 and its derivatives, respectively.

Pyr-actin was prepared by labeling actin with *N*-(1-pyrenyl)iodoacetamide according to ref *46* with modification as in ref *47* except that the gel-filtration Sephacryl 200 column was equilibrated with 5 mM HEPES, 50 μM ATP, and 0.1 mM CaCl$_2$, pH 8.0. The extent of labeling was determined by use of a molar extinction coefficient of $E_{344 nm} = 22\,000$ M^{-1}·cm^{-1} for the pyrene−protein complex (*48*).

Cross-Linking Experiments. Filamentous actin (30 μM) in cross-linking buffer (30 mM MOPS and 2.5 mM MgCl$_2$, pH 7.0) was mixed with the different motor domains at an actin: motor domain ratio of 5. The cross-linking reaction was initiated by addition of 15 mM NHS and EDC (freshly dissolved in the cross-linking buffer). For time course analysis, reactions were stopped before the addition of EDC or after the times indicated by the addition of Laemmli's buffer [50 mM HEPES, 2% (w/v) SDS, 1% β-mercapto-ethanol, and 50% (v/v) glycerol] and the content of the reaction mixture was analyzed by SDS−PAGE. Alternatively, the reactions were stopped after 20 min by the addition of 50 mM β-mercaptoethanol and 200 mM glycine and the covalent actin−motor domain complexes were digested by thrombin as described (*21*).

For cross-linking experiments performed in the presence of nucleotide analogues, the motor domains were preincubated for 15 min at room temperature with 2 mM ADP in the absence or in the presence of 10 mM NaF and 2 mM BeSO$_4$ for the formation of motor domain·ADP·BeF$_x$. Samples were electrophoresed on 4−18% gradient poly-acrylamide gels containing SDS (*49*).

---

[1] Abbreviations: EDC, 1-ethyl-3-[3-(dimethylamino)propyl]carbo-diimide; HEPES, *N*-(2-hydroxyethyl)piperazine-*N*′-2-ethanesulfonic acid; K_{app}, apparent K_M for actin; k_{cat}, maximum turnover rate in the presence of actin; K_d, k_{+A}, and k_{-A}, equilibrium, association rate, and dissociation rate constant of the actomyosin complex; M765, residues 1−765 of *Dictyostelium discoideum* myosin motor domain; M765(Sk) or M765(NM), chimeric constructs of M765 containing human skeletal muscle or human nonmuscle loop 3; MOPS, 3-(*N*-morpholino)-propanesulfonic acid; NHS, *N*-hydroxysuccinimide; PCR, polymerase chain reaction; pyr-actin, actin labeled with *N*-(1-pyrenyl)iodoacetamide on Cys-374; Sk-S1 or Sm-S1, myosin subfragment 1 from skeletal or smooth muscle; SDS−PAGE, sodium dodecyl sulfate−polyacrylamide gel electrophoresis.
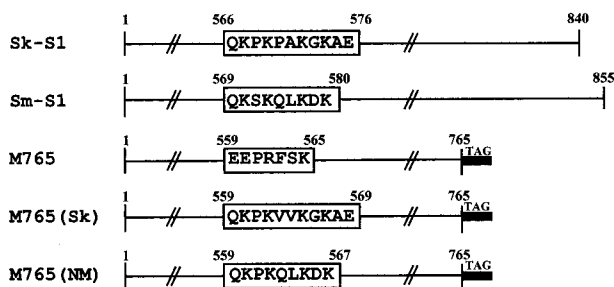
FIGURE 1: Schematic representation of the different myosin motor domains. The myosin motor domain of rabbit skeletal muscle (Sk-S1), chicken gizzard smooth muscle (Sm-S1), *D. discoideum* (M765), and the two chimeric constructs M765(Sk) and M765-(NM), in which *D. discoideum* myosin loop 3 is replaced by the sequence of human skeletal and nonmuscle myosin, respectively, are represented. All myosin molecules from *D. discoideum* have a C-terminal tag [Ala-Leu (His)$_8$].

Stopped-Flow Measurements. Stopped flow experiments were performed at a controlled temperature of 20 °C with a Hi-tech Scientific SF-61 or SF-61DX stopped-flow spectrophotometer. Pyrene fluorescence was excited at a wavelength of 365 nm and detected after passage through a KV 399 nm Schott filter on the emission beam. Transients shown were the average of 5−10 consecutive shots of the stopped-flow apparatus. All concentrations refer to the concentration of the reactants after mixing in the cell. The buffer used for all transient kinetic experiments was 20 mM MOPS, 5 mM MgCl$_2$, and 100 mM KCl, pH 7.0. Data were analyzed with the software GraphPad Prism.

Steady-State ATPase Assays. The actin-activated Mg^{2+}-ATPase activity was measured at 25 °C in 25 mM imidazole, 25 mM KCl, and 4 mM MgCl$_2$, pH 7.4, in the presence of 2 mM ATP. The amount of P$_i$ liberated was evaluated colorimetrically (50). Alternatively, the amount of ADP liberated was estimated by the pyruvate kinase−lactate dehydrogenase assay (20). Very comparable results were obtained independently of the method used.

RESULTS

We compared the actin binding properties of two sets of proteins that contained loop 3 segments varying in length, net charge and amino acid content. One set consisted of two myosin motor domains purified form rabbit skeletal and chicken gizzard myosin after chymotrypsin (Sk-S1) and papain (Sm-S1) digestion, respectively (Figure 1). The second set contained chimeric *D. discoideum* myosin motor domain constructs. Herein, the loop 3 region composed by residues 559−565 of wild-type M765 (EEPRFSK) was replaced by the corresponding sequence of human skeletal muscle myosin (QKPVVKGKAE) in M765(Sk) or human nonmuscle myosin (QKPKQLKDK) in M765(NM) (Figure 1). These three recombinant constructs were overexpressed in *D. discoideum* with a C-terminal His tag and purified by Ni-chelate chromatography (20).

Sequence Specificity of Myosin Loop 3 Binding to Actin. The specificity of actin binding to myosin loop 3 was assessed by cross-linking reaction mediated by EDC and NHS for two reasons: first, it uses a so-called zero length reagent that makes covalent contacts between adjacent amino acid side chains, and second, it is particularly well documented for the actomyosin complex both in the absence (25,

27, 51, 52) and in the presence of the ATP analogues (9). As depicted in Figure 2 (panel Sk-S1), three main cross-linking products with apparent molecular masses of 165, 175, and 265 kDa were generated when the cross-linking reaction was conducted at an actin/Sk-S1 molar ratio higher than 1. The 165 and 175 kDa products were found to contain one actin molecule cross-linked via its segment 1−12 to myosin loop 2 and loop 3, respectively (53, 54). The same segments of Sk-S1 were proposed to be cross-linked simultaneously to two actin monomers in the 265 kDa product (25, 52).

When the cross-linking reaction was conducted between actin and the smooth muscle motor domain (Sm-S1) or M765, a single cross-linked product of 160 or 145 kDa was observed (Figure 2). These products were also previously obtained with smooth muscle myosin in the absence of NHS (31) and with M765 (31). In both cases, they arose from the covalent attachment of actin to myosin loop 2. Even in the presence of NHS, which is known to dramatically increase the cross-linking yield, there was no band that could contain actin cross-linked to loop 3 of either Sm-S1 or M765 (Figure 2). To show that this lack of cross-linking was only due to the sequence of loop 3 and not to other structural differences between Sk-S1 and Sm-S1 or M765, we performed similar cross-linking experiments with M765, M765(Sk), and M765-(NM), which differ solely in their loop 3 sequence. In addition to the 145 kDa adduct obtained with M765, cross-linking of M765(Sk) to actin clearly revealed a new major product, migrating at 155 kDa (Figure 2). Cross-linking of M765(NM), in contrast, produced mainly the 145 kDa band with only traces of the new 155 kDa adduct. Note that with these two constructs, the 265 kDa band was weakly produced (Figure 2).

Since the 155 kDa adduct appeared only when the sequence of loop 3 was mutated, we concluded that it contains actin cross-linked to the mutated loop 3 of M765. Doublet bands of 145−155 kDa in the case of M765(Sk) and 165−175 kDa in the case of Sk-S1 were obtained. The faster migrating 145 and 165 kDa bands contained actin cross-linked to myosin loop 2 (21, 53, 54). The fact that the M765(Sk)-derived 155 kDa band contains actin cross-linked to myosin loop 3 is consistent with previous work that located the actin cross-linking site of the 175 kDa product within the 8 kDa stretch of residues (containing loop 3) at 27−35 kDa from the C-terminus of Sk-S1 (25, 55).

The actin residues cross-linked in the 155 kDa band were identified after depolymerization of the covalent products followed by thrombin treatment. Thrombin treatment does not cleave M765 but degrades monomeric actin independently of the presence of myosin at residues 28, 39, and 113, leading to actin peptides 40−375 (A37), 114−375 (A27), 40−113 (A10), 1−28, and 29−39 (21, 25, 56, 57). Figure 3 describes the electrophoresis pattern of the thrombin digestion of the 145 kDa product alone (obtained with the actin−M765 complex) or of a mixture of the 145, 155, and 265 kDa cross-linked products [produced with the actin−M765(Sk) and actin−M765(NM) complexes]. Thrombin treatment always resulted in a single band migrating with an apparent mass of 90 kDa (Figure 3, lanes c). The 90 kDa band arising from the 145 kDa covalent adduct was previously shown to contain actin peptide 1−28 linked to M765 (21). Thrombin treatment of all the EDC cross-linked products of the actomyosin complex generates a band of about 90 kDa (95 kDa for
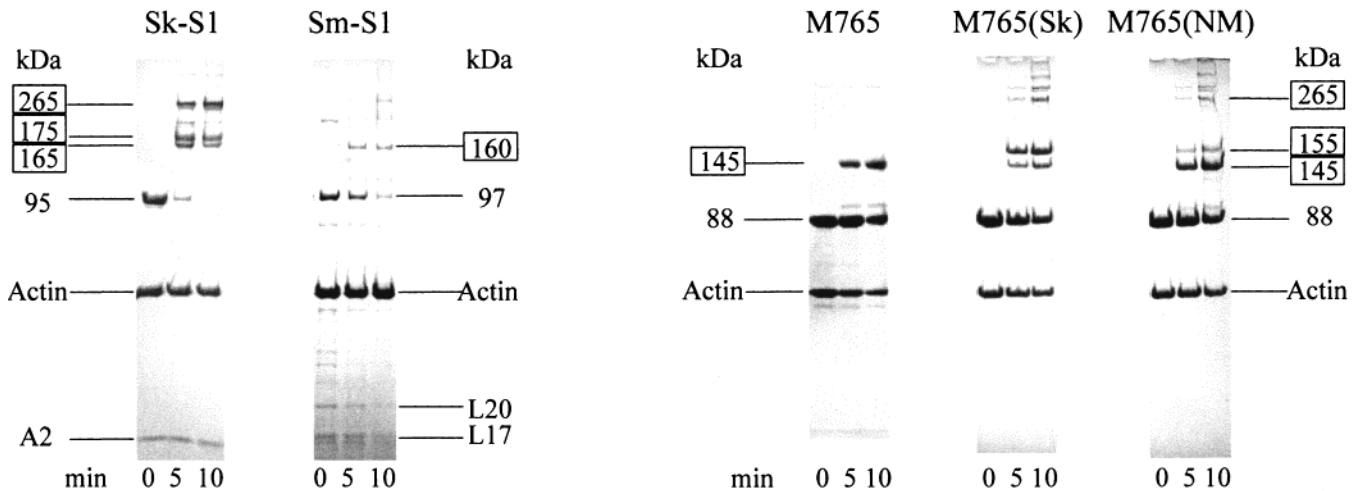
FIGURE 2: EDC-induced cross-linking of the motor domains to filamentous actin. Actin was cross-linked to Sk-S1, Sm-S1, M765, M765-(Sk), or M765(NM) as described under Materials and Methods. The samples were analyzed by gel electrophoresis after 0, 5, or 10 min of reaction. Cross-linked products are boxed.
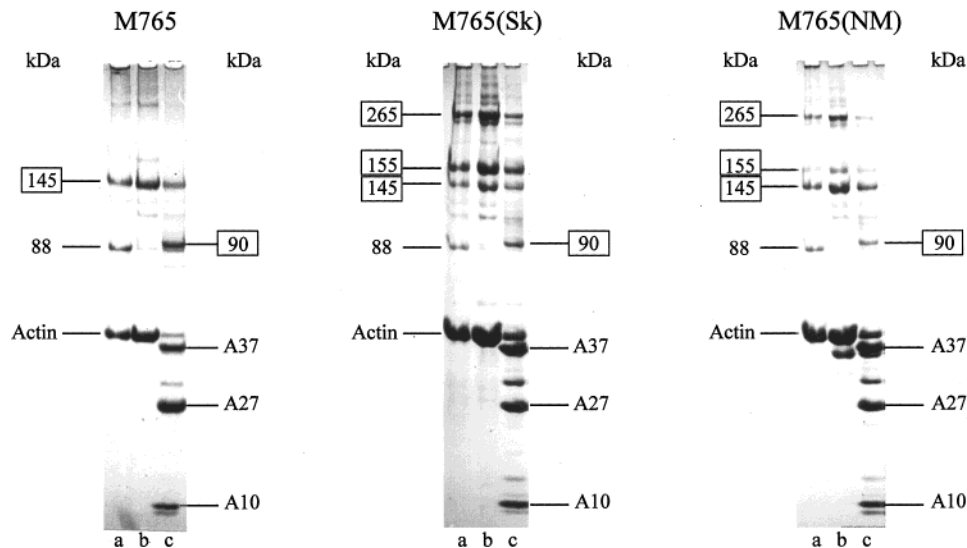

FIGURE 3: Identification of the actin cross-linking site. M765, M765(Sk), and M765(NM) were cross-linked to actin and subjected to thrombin cleavage as described under Materials and Methods. Cross-linked actin−motor domain complexes (lanes a) were depleted of un-cross-linked motor domain (lanes b) and digested by thrombin for 20 min (lanes c). A37, A27, and A10 are thrombin peptides of actin 40−375, 114−375, and 40−113, respectively. Cross-linked products are boxed.

skeletal muscle myosin) with the actin−peptide 1−28 bound to the motor domain (*21*, *58*). This result is in perfect agreement with the strong and very specific reactivity of the carboxylate residues of this 1−28 actin-derived peptide (*59*). By analogy with these results and using the arguments developed previously (*21*), we propose that the 90 kDa band issued from the 155 kDa (or the 265 kDa) adduct contains actin peptide 1−28 cross-linked to loop 3 of M765(Sk).

Nucleotides Effect on Myosin Loop 3 Binding to Actin. In the presence of the ATP analogues that stabilize the myosin·ADP·P_i intermediate state, the actin filament interacts simultaneously with loop 2 and loop 3 of Sk-S1, generating predominantly the 265 kDa covalent complex after the EDC cross-linking reaction (*9*). In the experiments depicted in Figure 4, we examined the effect of ADP·BeF$_x$ on the cross-linking pattern obtained between actin and M765, M765-(Sk), and M765(NM). First of all, control experiments performed in the presence of ADP (Figure 4, lanes a) generated electrophoretic gel patterns very similar to those obtained in the absence of nucleotide (Figure 2). This result

is in good agreement with the observation that ADP binding does not induce major modifications of the interface (*9*, *60*). The presence of ADP·BeF$_x$ did not affect the number or the size of the cross-linking products obtained with M765 (Figure 4, panel M765). However, the yield of the unique 145 kDa band was significantly reduced, probably due to ADP·BeF$_x$-induced dissociation of the actin−myosin complex (*61*). In contrast, when the reaction was performed with the mutated constructs M765(Sk) and M765(NM), the cross-linking pattern was strongly modified by ADP·BeF$_x$ [Figure 4, panels M765(Sk) and M765(NM)]. Among the three products of 145, 155, and 265 kDa that were observed in the presence of ADP, only the 265 kDa band was preferentially obtained with ADP·BeF$_x$. This nucleotide-induced cross-linking specificity is in good agreement with results recently obtained under similar conditions with the skeletal muscle myosin motor domain (*61*).

Role of Loop 3 in the Stabilization of the Actomyosin Complex. The binding of actin to Sk-S1 and *D. discoideum* myosin constructs was monitored by the change in pyrenyl-
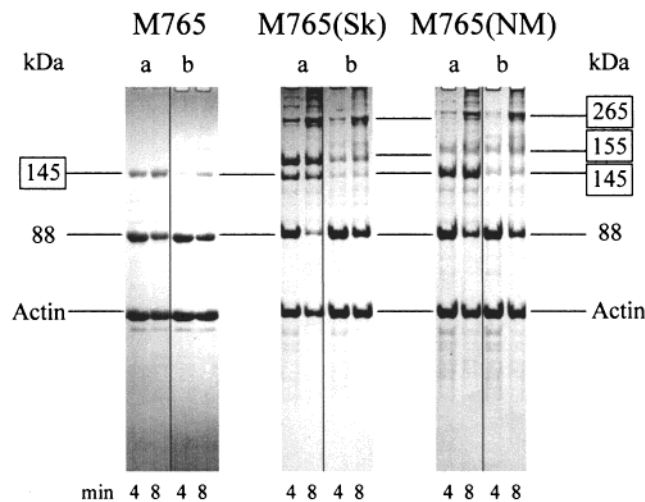
FIGURE 4: EDC-induced cross-linking in the presence of nucleotides. Cross-linking reactions were performed on 30 μM actin mixed with 10 μM M765, M765(Sk), or M765(NM) in the presence of 2 mM ADP (lanes a) or ADP·BeF$_x$ (lanes b) Aliquots were analyzed by gel electrophoresis after 4 or 8 min of reaction as described under Materials and Methods. Cross-linked products are boxed.

actin (pyr-actin) fluorescence (*48, 62*). Upon mixing of 0.5 μM motor domain constructs with increasing concentrations of pyr-actin (from 0.5 to 2.5 μM), an exponential decrease of the fluorescence was observed (Figure 5, inset). The transient records could be fitted by a single-exponential function for all the pyr-actin concentrations. The values of the observed rate constants (k_{obs}) were plotted versus pyr-actin concentration and showed a linear dependence over the concentration range studied (Figure 5). The second-order rate constants (k_{+A}) obtained from the gradients were 6.7 μM^{-1} s^{-1}, 1.4 μM^{-1} s^{-1}, 2.4 μM^{-1} s^{-1}, and 2.5 μM^{-1} s^{-1} for Sk-S1, M765, M765(Sk), and M765(NM), respectively.

The dissociation rates (k_{-A}) of the actomyosin complexes were determined by a displacement method in which pyr-actin is chased with an excess of unlabeled actin. Representative transients for displacement of pyr-actin from 0.5 μM pyr-actin−motor domain complexes mixed in a stopped-flow apparatus with 10 μM unlabeled actin are shown in Figure 6. The data were fitted with a single-exponential function leading directly to k_{-A}. Pyr-actin was displaced very quickly in the presence of Sk-S1 (<30 ms) with a k_{-A} of 0.187 s^{-1}, 25 times faster than with M765 (k_{-A} = 0.007 s^{-1}). The two chimeric constructs, M765(Sk) and M765(NM), showed a 8- and 6-fold increase in k_{-A} as compared with the wild-type M765 motor domain.

Loop 3 in the Pathway of ATP Binding and Hydrolysis by Actomyosin. Dissociation of the actomyosin complex by ATP was used to follow ATP binding to the myosin constructs in the presence of actin and the data were analyzed according to the two step model shown in Scheme 1. In this scheme, A and M represent actin and the myosin motor domain, respectively.

Scheme 1

$$\text{A·M} + \text{ATP} \xrightleftharpoons{K_1} \text{A·M·ATP} \xrightarrow{k_{+2}} \text{A} + \text{M·ATP} \rightarrow$$

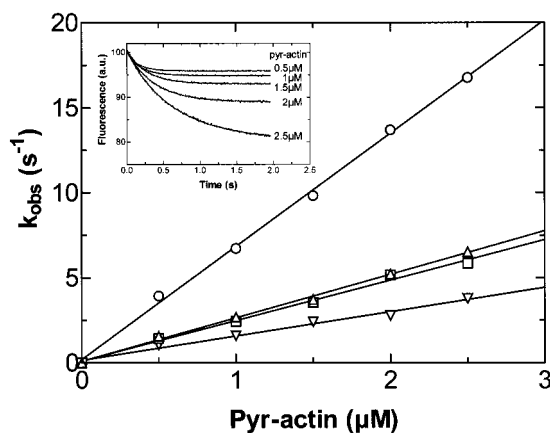The progress of the reaction was followed by measuring the increase in fluorescence of pyr-actin as dissociation

FIGURE 5: Rate of actin binding to the myosin motor domains. Increasing concentrations of pyr-actin (0.5−2.5 μM) were mixed with 0.5 μM Sk-S1 (○) M765 (▽), M765(Sk) (□) or M765(NM) (△) in the stopped-flow apparatus. Fluorescence change was monitored as described under Materials and Methods and fitted to a single-exponential function. The values of the observed rate constants (k_{obs}) were plotted versus the pyr-actin concentration. The second-order rate constants (k_{+A}) obtained from the slopes for Sk-S1, M765(Sk), M765(NM), and M765 were 6.7, 2.4, 2.5, and 1.4 μM^{-1}·s^{-1}, respectively. (Inset) Example of stopped-flow record obtained after mixing M765(NM) with increasing actin concentrations.
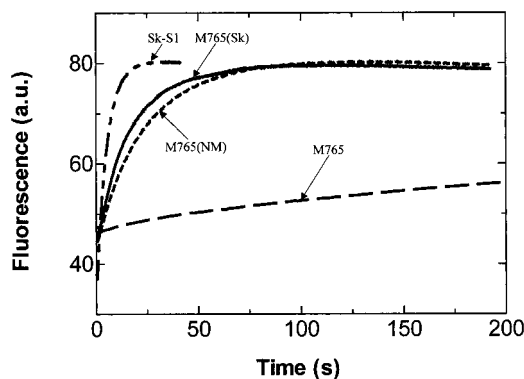

FIGURE 6: Actin-induced dissociation of the actin−motor domain complexes. pyr-actin−motor domain (0.5 μM) was mixed with 10 μM unlabeled actin in the stopped-flow apparatus. The fluorescence change was monitored during the time course of the displacement of pyr-actin from pyr-actin−Sk-S1 (−· −·), pyr-actin−M765(Sk) (—), pyr-actin−M765(NM) (- - -) or pyr-actin−M765 (− − −) as described under Materials and Methods. The data were fitted to a single exponential, defining values for dissociation rate constants (k_{-A}) of 0.187, 0.059, 0.043, and 0.007 s^{-1}, respectively.

occurred (Figure 7, inset). The rate of the observed single exponential (k_{obs}) was linearly dependent on ATP concentration from 1 to 5 μM (Figure 7). The slope of this plot defines the apparent second-order rate constant K_1k_{+2}, since for the two-step model

$$k_{obs} = K_1k_{+2}[\text{ATP}]/(1 + K_1[\text{ATP}])$$

For Sk-S1, the binding rate constant was 11-fold faster than for M765 (2.82 versus 0.26 μM^{-1} s^{-1}), in good accordance with the 12-fold difference previously reported between these two types of motor domain or the corresponding full-length myosins (*62, 63*). With the chimeric constructs, M765(Sk) and M765(NM), the binding rate of ATP was only slightly higher than with the parent M765 molecule
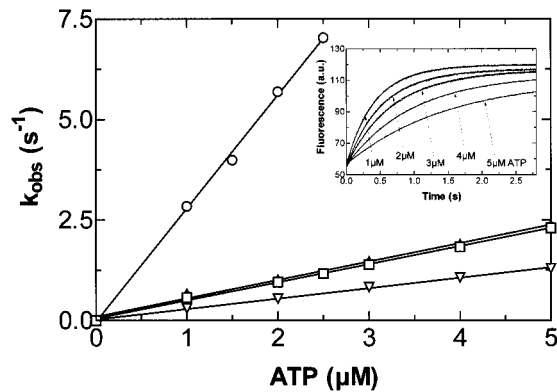
FIGURE 7: ATP-induced dissociation of actin−motor domain complexes. The change in pyrenyl fluorescence upon mixing 0.5 μM pyr-actin−motor domain complexes with an excess of ATP (1−5 μM) was monitored in the stopped-flow apparatus. The transient records were fitted by a single-exponential function and the observed rate constants (k_{obs}) were plotted versus the ATP concentration. The second-order rate constants were obtained from the slopes for Sk-S1 (○), M765(Sk) (□), M765(NM) (△), and M765 (▽) were 2.82, 0.45, 0.46, and 0.26 μM^{-1}·s^{-1}, respectively. (Inset) Example of fluorescence change observed upon mixing pyr-actin−M765(NM) complex with five different ATP concentrations.

(1.7-fold increased) independently of the origin of the primary sequence substituted in loop 3. The lack of dependence of the loop 3 sequence on ATP binding to myosin was confirmed in the absence of actin by monitoring the increase in intrinsic protein fluorescence following addition of ATP as described for M765 (*64*). We measured second-order rate constants of ATP binding (K_1k_{+2}) of 0.61 μM^{-1} s^{-1}, 0.71 μM^{-1} s^{-1}, and 0.64 μM^{-1} s^{-1} for M765, M765-(Sk), and M765(NM), respectively. The rate constant for the hydrolysis step was essentially invariant for all constructs, yielding 30 s^{-1} for M765, 36 s^{-1} for M765(Sk), and 22 s^{-1} for M765(NM) (data not shown).

ATP hydrolysis by the different constructs was measured over a large range of actin concentrations (data not shown). The ATPase activities of M765 and of its chimeric derivatives showed an almost linear dependence up to 100 μM actin as previously reported (*20*). Therefore, K_{app} was estimated to be greater than 100 μM for M765, M765(Sk), and M765(NM). For the same constructs, the maximum ATPase velocity, estimated at infinite actin concentration (k_{cat}), was 2.6 s^{-1}, 2.8 s^{-1}, and 2.9 s^{-1}, respectively. Under identical conditions, k_{cat} for Sk-S1 at infinite actin concentration was 4.6 s^{-1}.

DISCUSSION

Our results establish a clear correlation between the primary structure of myosin loop 3 and the binding of this loop to filamentous actin. They also show that this interaction apparently does not modulate the rate of ATP binding or that of ATP hydrolysis by the actin−myosin complex. These overall results are summarized in Table 1.

Actin Interacts Preferentially with Loop 3 of Striated Muscle Myosin. Among the five motor domains used in this study, only those containing loop 3 of skeletal muscle myosin can efficiently be cross-linked and therefore interact with actin. By comparing the actin cross-linking data with the loop 3 sequences, we can establish four criteria for actin interaction to occur. The number of net positive charges and

probably the length of the loop seem to be essential since M765, which does not cross-link through loop 3, has no net positive charges in its loop and is four residues shorter than loop 3 of Sk-S1 or M765(Sk), which does cross-link to actin. Charge distribution may also play an important role since loops 3 of M765(NM) and Sm-S1, which have 3 net positive charges but with one aspartate between two lysine residues, show very poor or no cross-linking. Finally, some flexibility of the loop 3 region seems to be required to make contact with the neighboring actin subdomain 1 possible. Sm-S1, which has almost the same loop 3 sequence as M765(NM) except for a serine-to-proline substitution, does not cross-link at all to actin. Therefore, this difference in cross-linking behavior can most likely be attributed to the reduced conformational flexibility of the Sm-S1 loop 3 region.

A careful analysis of the primary structure of loop 3 of myosin II isoforms reveals that only myosins from striated muscle seem to fulfill the criteria, in regard to charge content, charge distribution, length, and flexibility, needed for an optimal interaction with actin subdomain 1 (Figure 8). Accordingly, it was shown that loop 3 of both cardiac muscle (*27*) and scallop striated adductor muscle myosin (*65*) could cross-link to actin. Altogether, these results suggest that a specific and stable interaction between actin and myosin loop 3 is characteristic of striated muscle myosin.

Actin Binding to Myosin Loop 3 Occurs both in the Strong and in the Weak Binding States. It has been known for a long time that myosin binding to actin is specifically affected by the type of nucleotide with a decrease of 4 orders of magnitude in the affinity of actin when the ATP analogues are bound to the myosin active site (see for example refs *23*, *24*, *66*, and *67*). The case of myosin loop 2 is very peculiar since the presence of ATP analogues reduces only slightly its interaction with actin but also modifies the contributions of each lysine residue of loop 2 in the formation of the interface (*68−70*). The cross-linking results obtained with wild-type *D. discoideum* M765 are at least in partial agreement with these data since the presence of ATP analogues only decreases to a small extent actin cross-linking.

We recently found that skeletal muscle myosin loop 3 does also interact with actin in the weak binding complexes (*9*). This feature is totally confirmed in this study since in the presence of an ATP analogue both loop 2 and loop 3 of the *D. discoideum* chimeric constructs could cross-link to actin, generating predominantly the 265 kDa cross-linked product. This result fully agrees with the idea that myosin loop 2 and loop 3 (for striated muscle myosin) contribute significantly to the ionic contacts that still exist in the weak binding states, between actin and the myosin·ATP or myosin·ADP·P$_i$ intermediates (*9*). An interesting question raised by this work is the extent to which loop 3 contributes to the stabilization of these weak binding states. The fact that most myosins do not fulfill the criteria required for loop 3 interaction with actin suggests that this interaction may only have a stabilizing effect on the weak binding intermediates in the striated muscle actomyosin complexes.

Addition of Positive Charges in Loop 3 Destabilizes the Overall Interface between Actin and D. discoideum M765. The values of k_{+A} obtained for unmodified Sk-S1 and M765 (Table 1) are in good agreement with those reported previously under similar experimental conditions (*63*, *71*, *72*). It was proposed that the 4.8-fold difference in k_{+A} is due, at

Table 1: Actin and ATP Binding Properties of Different Myosin Motor Domains

					actin binding				ATP binding	ATP hydrolysis
	primary sequence	length	net charge	Pro content	cross-linking	k_{+A} (μM$^{-1}\cdot$s^{-1})	k_{-A} ($\times 10^2$ s^{-1})	$K_d{}^a$ (nM)	K_1k_{+2} (μM$^{-1}\cdot$s^{-1})	K_{cat} (s^{-1})
Sk-S1	QKPKPAKGKAE	11	+3	2	+	6.7	18.7	28.2	2.82	4.6
Sm-S1	QKSKQLKDK- -	9	+3	0	−	1.2^b	0.4^b	3.5^b	2.10^b	0.7^c
M765	EEPRFSK- - - -	7	0	1	−	1.4	0.7	4.6	0.26	2.6
M765(Sk)	QKPKVVKGKAE	11	+3	1	+	2.4	5.9	25.0	0.45	2.8
M765(NM)	QKPKQLKDK- -	9	+3	1	− (+)	2.5	4.3	16.9	0.46	2.9

^{a} $K_d = k_{-A}/k_{+A}$. ^{b} As reported in ref *74* at 20 °C in 20 mM MOPS, pH 7.0, 0.1M KCl, 1 mM DTT, 0.1 mM EGTA, and 5 mM MgCl$_2$. ^{c} From ref *75* at 25 °C in 5 mM Tris, pH 7.0, 10 mM KCl, and 3 mM MgCl$_2$.

```
Striated muscle   QKP-KPAKGKAE        RabSk
                  QKP-KVVKGKAE        HumFSk
                  QKP-RNVKGKQE        RatCα
                  QKP-RNIKGKQE        RatCß
                  QKP-RNIKGKPE        HumCα+ß
                  TKPGKPTRPNQG        ScalSt
                  QKP-KPPKPGQQ        DmM
                  EKP-KPPKGKQG        CeMB
                  QKP-KPPKGKQG        CeMA

Smooth muscle     QKS-KQLKDK--        ChkSm
                  QKP-KQLKDK--        RabSm

Nonmuscle         QKP-KQLKDK--        HumNMA
                  QKP-RQLKDK--        HumNMB
                  MKT-----DFRG        DmNM
                  EEP-RFSK----        DdII
                  RRP-RF--DA--        AcII
                  RKP-RIGGDGV-        EhII
                  KRS--ALK----        ScII
```

FIGURE 8: Primary sequence alignment of the secondary actin binding sites of different myosin II. The partial primary sequences of the myosin II isoforms were extracted from Goodson and Sellers (*3*).

least in part, to the additional positive charges present in the loop 2 segment of Sk-S1 (*20*). Replacement of the loop 3 region of M765 with human skeletal muscle or nonmuscle myosin-derived loop 3 sequences induces a 1.8-fold increase in k_{+A}, demonstrating that additional positive charges in loop 3 contributes to the higher actin binding rate obtained with skeletal muscle myosin (Table 1). Surprisingly, with the same substitutions of *D. discoideum* loop 3 we observed a 6−8-fold increase in actin dissociation rate, k_{-A}. This increase in k_{-A} can only be explained by a destabilization of the natural actin−*D. discoideum* myosin contact as suggested by the large difference in the values of K_d calculated from the ratios k_{-A}/k_{+A} (Table 1). One interpretation is that strengthening the secondary actin binding site could slightly distort and destabilize the overall rigor complex.

The Structure of Loop 3 Is Not Essential for ATP Binding or ATP Hydrolysis by the Actomyosin Complex. A large difference in ATP binding and ATP hydrolysis parameters does exist between muscle and nonmuscle myosin II. However, there are no significant changes in these parameters upon substitution of loop 3 segment in M765 (Table 1). These results are quite surprising since loop 3 of the chimeric constructs interacts with actin both in the rigor actomyosin complex and in the weak actin−myosin·ADP·P$_i$ intermediate. It looks like the binding energy utilized for this additional interface and present only in striated muscle myosin isoforms is not at all related to the actin-induced ATPase activation process. In agreement with the lack of a functional role of loop 3 in the actin-activated ATPase activity, no difference

in the activity was found when the accessibility of loop 3 was hindered either by changing the degree of saturation of the actin filaments by myosin (*73*) or by antibodies directed against skeletal muscle myosin loop 3 (*30*). Furthermore, our results suggest that only the loop 3 region of striated muscle myosins has a modulating effect on the interaction with actin. Further experiments are now underway to determine whether this loop 3 region also modulates the displacement velocity of striated muscle myosin along the thin filaments.

REFERENCES

1. Fisher, A. J., Smith, C. A., Thoden, J. B., Smith, R., Sutoh, K., Holden, H. M., and Rayment, I. (1995) *Biochemistry 34*, 8960−8972.
2. Houdusse, A., Kalabokis, V. N., Himmel, D., Szent-Gyorgyi, A. G., and Cohen, C. (1999) *Cell 97*, 459−470.
3. Sellers, J. R., and Goodson, H. V. (1995) *Protein Profile 2*, 1323−1423.
4. Cope, M. J. T., Whisstock, J., Rayment, I., and Kendrick-Jones, J. (1996) *Structure 4*, 969−987.
5. Rayment, I., Holden, H. M., Whittaker, M., Yohn, C. B., Lorenz, M., Holmes, K. C., and Milligan, R. A. (1993) *Science 261*, 58−65.
6. Schroder, R. R., Manstein, D. J., Jahn, W., Holden, H., Rayment, I., Holmes, K. C., and Spudich, J. A. (1993) *Nature 364*, 171−174.
7. Highsmith, S., and Murphy, A. J. (1992) *Biochemistry 31*, 385−389.
8. Geeves, M. A., and Conibear, P. B. (1995) *Biophys. J. 68*, 194S−199S.
9. Van Dijk, J., Fernandez, C., and Chaussepied, P. (1998) *Biochemistry 37*, 8385−8394.
10. Wong, W. W., Doyle, T. C., and Reisler, E. (1999) *Biochemistry 38*, 1365−1370.
11. Chaussepied, P., and Van Dijk, J. (1999) *Molecular Interactions of Actin*, Springer-Verlag (in press).
12. Perreault-Micale, C. L., Kalabokis, V. N., Nyitray, L., and Szent-Gyorgyi, A. G. (1996) *J. Muscle Res. Cell Motil. 17*, 543−553.
13. Murphy, C. T., and Spudich, J. A. (1998) *Biochemistry 37*, 6738−6744.
14. Sweeney, H. L., Rosenfeld, S. S., Brown, F., Faust, L., Smith, J., Xing, J., Stein, L. A., and Sellers, J. R. (1998) *J. Biol. Chem. 273*, 6262−6270.
15. Spudich, J. A. (1994) *Nature 372*, 515−518.
16. Goodson, H. V., Warrick, H. M., and Spudich, J. A. (1999) *J. Mol. Biol. 287*, 173−185.

17. Chaussepied, P., and Morales, M. F. (1988) *Proc. Natl. Acad. Sci. U.S.A. 85*, 7471−7475.

18. Bobkov, A. A., Bobkova, E. A., Lin, S. H., and Reisler, E. (1996) *Proc. Natl. Acad. Sci. U.S.A. 93*, 2285−2289.

19. Uyeda, T. Q., Ruppel, K. M., and Spudich, J. A. (1994) *Nature 368*, 567−569.

20. Furch, M., Geeves, M. A., and Manstein, D. J. (1998) *Biochemistry 37*, 6317−6326.

21. Van Dijk, J., Furch, M., Derancourt, J., Batra, R., Knetsch, M. L., Manstein, D. J., and Chaussepied, P. (1999) *Eur. J. Biochem. 260*, 672−683.

22. Murphy, C. T., and Spudich, J. A. (1999) *Biochemistry 38*, 3785−3792.

23. Schreiber, G., and Fersht, A. R. (1996) *Nat. Struct. Biol. 3*, 427−431.

24. Tsai, C. J., Lin, S. L., Wolfson, H. J., and Nussinov, R. (1996) *Crit. Rev. Biochem. Mol. Biol. 31*, 127−152.

25. Bonafe, N., and Chaussepied, P. (1995) *Biophys. J. 68*, 35S−43S.

26. Andreev, O. A., Takashi, R., and Borejdo, J. (1995) *J. Muscle Res. Cell Motil. 16*, 353−367.

27. Andreev, O. A., and Borejdo, J. (1997) *Circ. Res. 81*, 688−693.

28. Chaussepied, P., Mornet, D., Audemard, E., Derancourt, J., and Kassab, R. (1986) *Biochemistry 25*, 1134−1140.

29. Szentkiralyi, E. M. (1987) *J. Muscle Res. Cell Motil. 8*, 349−357.

30. Blotnick, E., Miller, C., Groschel-Stewart, U., and Muhlrad, A. (1995) *Eur. J. Biochem. 232*, 235−240.

31. Marianne-Pepin, T., Mornet, D., Bertrand, R., Labbe, J. P., and Kassab, R. (1985) *Biochemistry 24*, 3024−3029.

32. Giese, K. C., and Spudich, J. A. (1997) *Biochemistry 36*, 8465−8473.

33. Eisenberg, E., and Kielley, W. W. (1974) *J. Biol. Chem. 249*, 4742−4748.

34. Offer, G., Moos, C., and Starr, R. (1973) *J. Mol. Biol. 74*, 653−676.

35. Weeds, A. G., and Taylor, R. S. (1975) *Nature 257*, 54−56.

36. Lheureux, K., Forne, T., and Chaussepied, P. (1993) *Biochemistry 32*, 10005−10014.

37. Marianne-Pepin, T., Mornet, D., Audemard, E., and Kassab, R. (1983) *FEBS Lett. 159*, 211−216.

38. Manstein, D. J., and Hunt, D. M. (1995) *J. Muscle Res. Cell Motil. 16*, 325−332.

39. Sambrook, J., and Gething, M. J. (1989) *Nature 342*, 224−225.

40. Braman, J., Papworth, C., and Greener, A. (1996) *Methods Mol. Biol. 57*, 31−44.

41. West, J. J., Nagy, B., and Gergely, J. (1967) *J. Biol. Chem. 242*, 1140−1145.

42. Wagner, P. D., and Weeds, A. G. (1977) *J. Mol. Biol. 109*, 455−470.

43. Godfrey, J. E., and Harrington, W. F. (1970) *Biochemistry 9*, 886−893.

44. Okamoto, Y., and Sekine, T. (1978) *J. Biochem. (Tokyo) 83*, 1375−1379.

45. Bradford, M. M. (1976) *Anal. Biochem. 72*, 248−254.

46. Cooper, J. A., Walker, S. B., and Pollard, T. D. (1983) *J. Muscle Res. Cell Motil. 4*, 253−262.

47. Lheureux, K., and Chaussepied, P. (1995) *Biochemistry 34*, 11435−11444.

48. Kouyama, T., and Mihashi, K. (1981) *Eur. J. Biochem. 114*, 33−38.

49. Laemmli, U.K. (1970) *Nature 227*, 680−685.

50. Mornet, D., Bertrand, R. U., Pantel, P., Audemard, E., and Kassab, R. (1981) *Biochemistry 20*, 2110−2120.

51. Grabarek, Z., and Gergely, J. (1990) *Anal. Biochem. 185*, 131−135.

52. Andreev, O., and Borejdo, J. (1992) *Biochem. Biophys. Res. Commun. 188*, 94−101.

53. Sutoh, K. (1982) *Biochemistry 21*, 3654−3661.

54. Sutoh, K. (1983) *Biochemistry 22*, 1579−1585.

55. Sutoh, K. (1982) *Biochemistry 21*, 4800−4804.

56. Muszbek, L., Gladner, J. A., and Laki, K. (1975) *Arch. Biochem. Biophys. 167*, 99−103.

57. Bertrand, R., Chaussepied, P., Kassab, R., Boyer, M., Roustan, C., and Benyamin, Y. (1988) *Biochemistry 27*, 5728−5736.

58. Bertrand, R., Chaussepied, P., Audemard, E., and Kassab, R. (1989) *Eur. J. Biochem. 181*, 747−754.

59. Elzinga, M. (1987) *Methods in Protein Science Analysis* (Walsh, K. E., Ed.) pp 615−623, Humana Press, Totowa, NJ.

60. Jontes, J. D., and Milligan, R. A. (1997) *J. Cell Biol. 139*, 683−693.

61. Van Dijk, J., Fernandez, C., and Chaussepied, P. (1998) *Biochemistry 37*, 8385−8394.

62. Ritchie, M. D., Geeves, M. A., Woodward, S. K., and Manstein, D. J. (1993) *Proc. Natl. Acad. Sci. U.S.A. 90*, 8619−8623.

63. Kurzawa, S. E., Manstein, D. J., and Geeves, M. A. (1997) *Biochemistry 36*, 317−323.

64. Furch, M., Fujita-Becker, S., Geeves, M. A., Holmes, K. C., and Manstein, D. J. (1999) *J. Mol. Biol. 290*, 797−809.

65. Hue, H. K., Labbe, J. P., Harricane, M. C., Cavadore, J. C., Benyamin, Y., and Roustan, C. (1988) *Biochem. J. 256*, 853−859.

66. Eisenberg, E., Zobel, C. R., and Moos, C. (1968) *Biochemistry 7*, 3186−3194.

67. Rovner, A. S., Freyzon, Y., and Trybus, K. M. (1995) *J. Biol. Chem. 270*, 30260−30263.

68. Chen, T., Applegate, D., and Reisler, E. (1985) *Biochemistry 24*, 5620−5625.

69. Arata, T. (1986) *J. Mol. Biol. 191*, 107−116.

70. Yamamoto, K. (1989) *J. Mol. Biol. 209*, 703−709.

71. Marston, S. B. (1982) *Biochem. J. 203*, 453−460.

72. Coates, J. H., Criddle, A. H., and Geeves, M. A. (1985) *Biochem. J. 232*, 351−356.

73. Lheureux, K., and Chaussepied, P. (1995) *Biochemistry 34*, 11445−11452.

74. Cremo, C. R., and Geeves, M. A. (1998) *Biochemistry 37*, 1969−1978.

75. Marston, S., and Taylor, E. (1980) *J. Mol. Biol. 139*, 573−600.